



HAL
open science

Detoxification of V-Nerve Agents Assisted by a Microperoxidase: New Pathway Revealed by the Use of a Relevant VX Simulant

Valmir Baptista da Silva, Jean-Pierre Mahy, Xavier Brazzolotto, Pierre-yves Renard, Rémy Ricoux, Julien Legros

► To cite this version:

Valmir Baptista da Silva, Jean-Pierre Mahy, Xavier Brazzolotto, Pierre-yves Renard, Rémy Ricoux, et al.. Detoxification of V-Nerve Agents Assisted by a Microperoxidase: New Pathway Revealed by the Use of a Relevant VX Simulant. *ChemBioChem*, 2024, 25 (15), pp.e202400137. <10.1002/cbic.202400137>. <hal-05500338>

HAL Id: hal-05500338

<https://hal.science/hal-05500338v1>

Submitted on 9 Feb 2026

HAL is a multi-disciplinary open access archive for the deposit and dissemination of scientific research documents, whether they are published or not. The documents may come from teaching and research institutions in France or abroad, or from public or private research centers.

L'archive ouverte pluridisciplinaire HAL, est destinée au dépôt et à la diffusion de documents scientifiques de niveau recherche, publiés ou non, émanant des établissements d'enseignement et de recherche français ou étrangers, des laboratoires publics ou privés.



Distributed under a Creative Commons CC BY 4.0 - Attribution - International License

Detoxification of V-Nerve Agents Assisted by a Microperoxidase: New Pathway Revealed by the Use of a Relevant VX Simulant

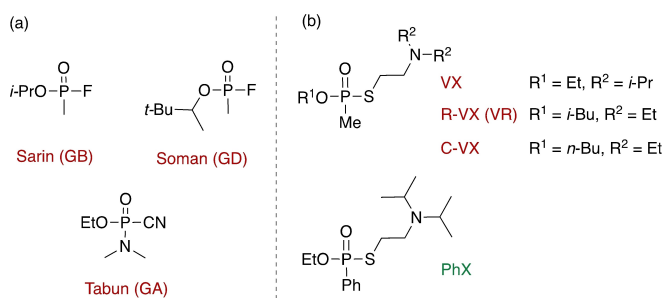
Valmir Baptista da Silva,^[a] Jean-Pierre Mahy,^[b] Xavier Brazzolotto,^[c] Pierre-Yves Renard,^[a] Rémy Ricoux,^{*[b]} and Julien Legros^{*[a]}

The biocatalyzed oxidative detoxification of the V-series simulant PhX, by mean of the microperoxidase AcMP11, affords the corresponding phosphonothioate as the prominent product instead of the classical P–S and P–O bond cleavage. While PhX is structurally very close to the live agent VX (the methyl group is replaced by a phenyl), assessment with other surrogates missing the nucleophilic amino function displayed more resistance under the same conditions with no phosphono-

thioate observed. These encouraging results highlight 1) the efficacy of AcMP11 microperoxidase to efficiently detoxify V-series organophosphorus nerve agents (OPNA), and 2) the necessity to use representative alkyl or aryl phosphonothioates simulants such as PhX bearing the appropriate side chain as well as the P–O and P–S cleavable bond to mimic accurately the V-series OPNA to prevent false positive or false negative results.

Introduction

Chemical warfare agents (CWA) remain a serious threat despite the implementation of the Chemical Weapon Convention: several cases of use with fatal consequences on individuals have been reported in recent years in various countries^[1–3] and tens of thousands of old chemical weapon items are still officially declared.^[4] Among CWA, organophosphorus nerve agents (OPNA) are extremely dangerous, and exposure leads to rapid death.^[5–8] The toxicity of the most common G-series OPNA (sarin, cyclosarin, tabun, soman, ...) relies primarily on the weakness of the P–F bond (or P–CN for tabun; Scheme 1a).^[9] G-agents quickly act with irreversible consequences on neurotransmission through inhibition of a key nerve impulse regulatory enzyme, namely acetylcholinesterase (AChE), but are volatile and quickly hydrolyzed in the environment and represent a non-persistent threat. In contrast, for the V-agents, the P(O)–S–(CH₂)₂–N(Alk)₂ key motif provides both greater toxicity and improved stability: this motif perfectly simulates



Scheme 1. Organophosphorus nerve agents: (a) G-series agents. (b) V-series agents (red) and PhX as simulant of VX (green).

acetylcholine while offering a moderate leaving group ability, and therefore a good stability toward hydrolysis (Scheme 1b).^[10,11] Moreover, while direct hydrolysis is the usual way to neutralize the most common G-series OPNA (due to the labile F/CN atom/group) V-series agents are reluctant to this detoxification path.^[6,12,13] Hydrolysis of the famous VX agent even affords two distinct organophosphorus molecules with opposite bioactivities depending on the cleavage site. When the P–S bond is cleaved, the harmless –and desired– ethyl methylphosphonic acid EMPA 1 is formed while the P–O bond cleavage yields the still very toxic and stable thiophosphonic acid EA-2192 2 (Scheme 2a).^[14] In 1990, Yang reported that the oxidation-assisted hydrolysis of VX was a powerful tool for the selective P–S bond cleavage of VX through oxidation of the sulfur atom (Scheme 2a).^[12,15] Thus, the application of an acidic aqueous solution of Oxone® (2KHSO₅KHSO₄K₂SO₄), allowed detoxification into the harmless product 1 along with the formation of the corresponding aminosulfonic acid through selective oxygen transfer onto the S atom (Scheme 2b).^[12,15] In contrast, under fully organic conditions (3-chloroperoxybenzoic acid, *m*-CPBA, in organic solvent), the *N*-oxide 4 was obtained. The latter further underwent a Cope elimination to yield the

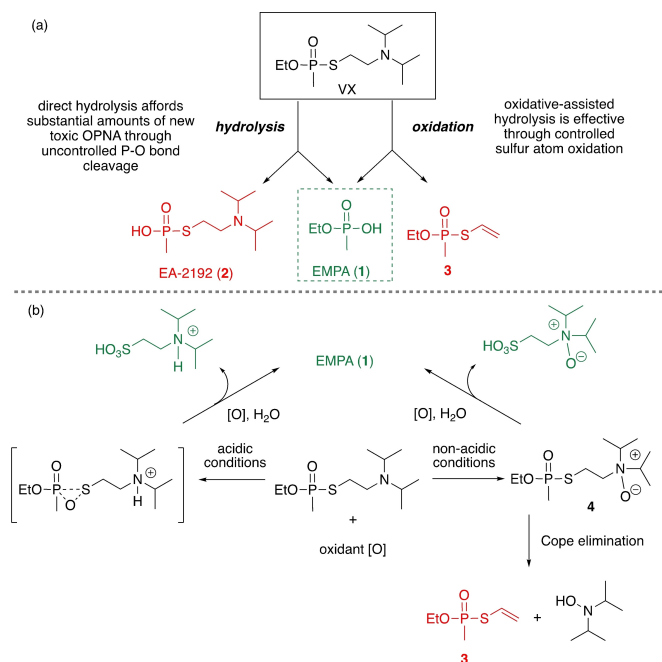
[a] Dr. V. B. da Silva, Prof. P.-Y. Renard, Dr. J. Legros
Univ Rouen Normandie, INSA Rouen Normandie, CNRS, Normandie Univ,
COBRA, F-76000 Rouen, France
E-mail: julien.legros@univ-rouen.fr

[b] Prof. J.-P. Mahy, Dr. R. Ricoux
Université Paris-Saclay, CNRS, Institut de Chimie Moléculaire et des
Matériaux d'Orsay, 91400, Orsay, France
E-mail: remy.ricoux@universite-paris-saclay.fr

[c] Dr. X. Brazzolotto
Département de Toxicologie et Risques Chimiques, Institut de Recherche
Biomédicale des Armées, 91220, Brétigny-sur-Orge, France

Supporting information for this article is available on the WWW under
<https://doi.org/10.1002/cbic.202400137>

© 2024 The Authors. ChemBioChem published by Wiley-VCH GmbH. This is an open access article under the terms of the Creative Commons Attribution License, which permits use, distribution and reproduction in any medium, provided the original work is properly cited.



Scheme 2. (a) Hydrolytic and oxidative decomposition paths of the VX agent. (b) Detailed mechanism of the oxidative-assisted decomposition of VX. Green = harmless, red = toxic.

toxic vinyl thiophosphonate **3** ($t_{1/2}$ (**4**) = 2 h at 20 °C) as depicted in Scheme 2b.^[12,15] However, by rapidly engaging **4** with an excess of *m*-CPBA in aq. *tert*-butanol, **4** was reported to afford the desired EMPA **1** along with the non-toxic *N*-oxide form of the aminosulfonic acid (Scheme 2b).^[12,15]

In the frame of the development of sustainable tools for the neutralization of CWA, it is highly desirable to replace Oxone® or *m*-CPBA with oxidants that generate as little effluents as possible.^[16,17] In this sense, hydrogen peroxide (H₂O₂) appears as the optimal reagent since it only releases water as effluent. The widely available 30% aqueous H₂O₂ (v/v) is inexpensive, stable, and easy to handle.^[18] However, the drawback of this stability is that the presence of an additional activating partner (ideally in a catalytic amount) in the reaction medium is required for the oxidation to occur.^[18] For such a purpose, enzymes are very attractive catalysts that encompass green requirements.^[19–21] Whereas the biocatalyzed decomposition of V-series OPNA has been mostly studied using phosphotriesterases,^[22–27] some scarce examples of chloroperoxidase have also been described.^[28] Yet catalytic efficiencies are to date too low, and enzyme production costs too high to allow practical use of these enzymes. The low substrate tolerance and poor water solubility of V-agents also limit the practical use of these enzymes. Among peroxidases, microperoxidases are small and cost-effective heme peptides obtained by proteolytic digestion of cytochrome *c*. Among them, microperoxidase 11 (MP11, Figure 1a) contains the protein segment 11–21 of cytochrome *c*. The heme is attached to the peptide via thioether linkages involving the thiol functions of the Cys14 and Cys17 side chains. The imidazole group of the side chain of His18 acts as the axial proximal ligand of the heme iron(III) ion whereas a water

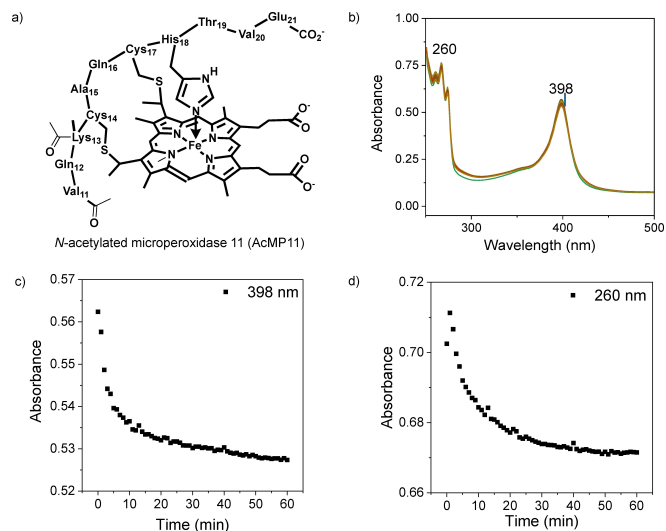


Figure 1. a) *N*-Acetylated microperoxidase-11; b) UV-visible spectra of a reaction mixture of AcMP11 (5 μM), PhX (500 μM), and H₂O₂ (50 μM) in MeOH/buffer pH 8 60/40; c) UV-monitored evolution of AcMP11 (398 nm), d) UV-monitored evolution of PhX (260 nm) under oxidative conditions A.

molecule or an exogenous ligand such as cyanide, halide, or an amine can act as its distal axial ligand. Microperoxidases display a peroxidase activity, meaning that they catalyze the reduction of hydrogen peroxide to water while oxidizing with high versatility and substrate tolerance to a numerous range of co-substrates such as ABTS, and *o*-dianididine pyrogallol. They also display monooxygenase-like activity, as they can catalyze sulfide oxidation, amine *N*-demethylation, olefin oxidation, and aniline *p*-hydroxylation.^[2,13–16] These reactions occur through a high valent heme iron-oxo intermediate –or ferryl species–, that arises from the reaction of either dioxygen in the presence of a reductant, or of H₂O₂, or other oxygen-atom donors with the iron(III) heme. This highly reactive species is responsible for the transfer of an oxygen atom to the substrates mentioned above.

Herein, we report the neutralization of a VX simulant by an oxidative process involving H₂O₂ as an oxidant and microperoxidase 11 as a catalyst.

Results and Discussion

For obvious safety, regulatory, and security issues, the use of real CWA is prohibited in academic laboratories and the substitution of VX by a simulant perfectly mimicking its behavior is required. In this line, the PhX molecule, developed by Renard and Mioskowski,^[29] is certainly the closest alternative to VX among all others.^[30–32] PhX only differs from the real CWA by a phenyl group in place of the non-reactive methyl group; which causes a reduction of the IC₅₀ value for AChE by 60-fold as compared to that of VX, with negligible aging phenomenon (Scheme 1b).^[29]

Due to the poor water solubility of V-agents (and related simulants) and limited compatibility of AcMP11 with organic media (as well as pH requirements), a balance had to be found

on the nature of the reaction medium to study the microperoxidase-catalyzed oxidative decomposition of PhX. Due to the structure of the compounds studied, UV-monitoring appears as a convenient method to study the stability/decomposition of PhX ($\lambda=260$ nm; Figure 1b) and MP-11 ($\lambda=398$ nm; Figure 1b). Assessment of conditions revealed that a medium buffered at pH 8 with 20 mM HEPES (2-[4-(2-hydroxyethyl)piperazin-1-yl]ethane-1-sulfonic acid) with a methanol content of 40% were the most satisfactory oxidation conditions to keep catalyst stability with simple commercial 30% aqueous H_2O_2 solution ($[\text{H}_2\text{O}_2]=250$ μM and $[\text{AcMP11}]=5$ μM , no PhX; see Supporting Information). Degradation experiments were thus performed by portion-wise addition of H_2O_2 over the buffered solution of PhX and AcMP11 (conditions A). Monitoring of the absorbance at 398 nm (AcMP11) and 260 nm (PhX) showed the effectiveness of the conditions with a significant decrease of the PhX concentration over 1 h (Figure 1d), accompanied by an expected (but slow) decomposition of the peroxidase (Figure 1c).

As mentioned above, the effective decomposition of CWA not only relies on the amount of toxic compound transformed but also on full identification of each compound formed during the reaction, since several products with opposite bioactivities can be produced. Thus, to ensure the decomposition of PhX into acceptable non-toxic compounds, the reaction was also monitored by $^{31}\text{P}\{^1\text{H}\}$ NMR, a powerful analytical method that provides in-depth information on the evolution of the reaction medium since each P-compound is characterized by a unique signal (Figure 2).

Surprisingly, these analyses revealed the formation of an early product, formed at $t=0$ (start of H_2O_2 addition), characterized by a signal at $\delta=67$ ppm distinct from the signals due to any of the expected products or starting material: PhX ($\delta=50$ ppm), the undesired P–O bond cleavage product **6** ($\delta=33$ ppm) and the target ethyl phenyl phosphinic acid product **7** ($\delta=16$ ppm). This signal was attributed to product **5a**. Monitoring of the reaction showed a regular increase of the amount of **5a** until $t=5$ h, accompanied by the late formation of products **6** and **7** from $t=2$ h, yet in limited amounts. The slow formation of these two latter products likely comes *a priori* from the classical competitive uncatalyzed decomposition paths of PhX through (per)hydrolysis.^[33–35] Regarding the structure of **5a**, its characteristic signal observed at $\delta=67$ ppm in ^{31}P NMR suggested that it belonged to the phosphonothioate $\text{R}(\text{RO})_2\text{P}=\text{S}$ series,^[36,37] which was then confirmed by comparison with the ^{31}P NMR spectrum of an authentic sample of $\text{Ph}(\text{OH})(\text{EtO})\text{P}=\text{S}$.

It was already reported in 1996 that such a harmless phosphonothioate could be formed from VX through a minor decomposition pathway in aqueous medium at high temperature over 1 week: expected products **1** and **2** were obtained along with traces of the related phosphonothioate product **5b**. The formation of **5b** likely occurs through N-assisted S–C bond cleavage of VX with the release of an aziridinium moiety **8** (Scheme 3).^[38] This transformation was reported later to be also promoted over sand,^[39] asphalt,^[36] or concrete.^[40] More recently, Kubik described that, in a basic D_2O medium (pD ca. 10), cyclic cucurbiturils (2 equiv.) promoted almost exclusively this reac-

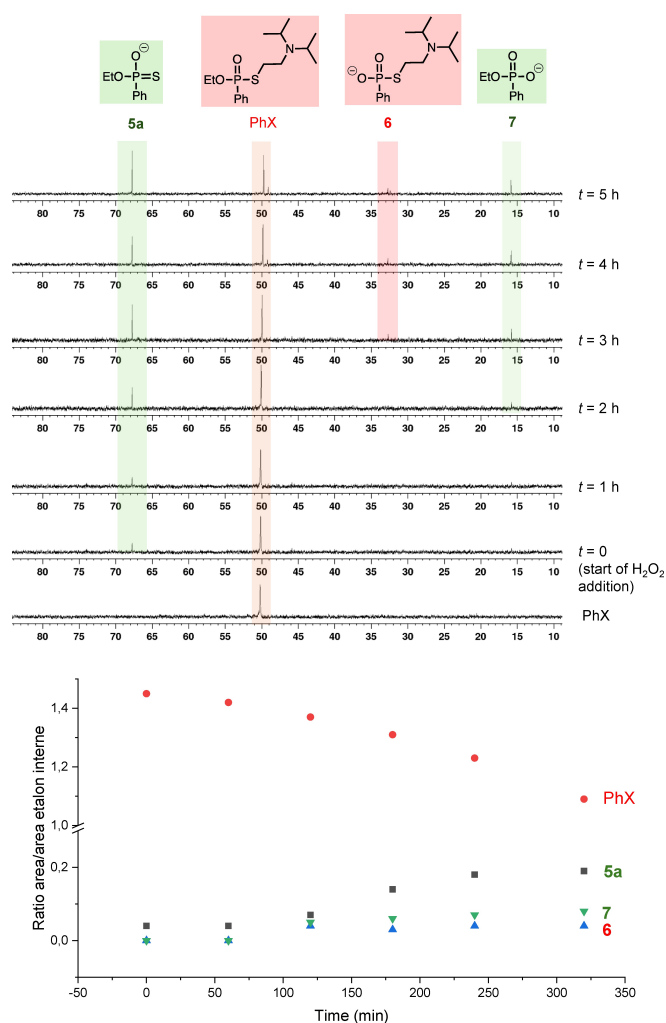


Figure 2. Monitoring of AcMP-11-catalyzed detoxification of PhX with H_2O_2 (conditions A). Top: ^{31}P NMR spectra. Bottom: evolution of concentration for each species.



Scheme 3. Formation of phosphonothioate **5** from V-series agents.

tion with the full conversion of VX into *O*-ethylmethyl phosphonothioate **5b** within ca. 30 min.^[37] Experimental and theoretical investigations suggested that cucurbiturils control the pre-organization of VX to favor aziridinium extrusion.

However, in our case, the reason for such specific behavior of PhX under oxidative conditions was unclear, and further studies were required. Experiments performed in aqueous buffered solution/methanol (60:40, pH 8) in the sole presence of 1 equiv. of H_2O_2 (conditions B) showed the slow formation of product **7** only (25% within 5 h), which confirmed the

hypothesis of a non-catalyzed competitive path. Finally, blank experiments in aqueous buffered solution/methanol (conditions C) did not show any transformation of PhX within 5 h, whereas several products appeared after 3 days (16% conversion of PhX into **5a**, **6** and **7** accompanied by the methanolysis of PhX into ethyl methyl phenylphosphonate).^[41]

From these results, it appears that the rapid formation of **5a** from PhX is only due to the microperoxidase activity in the presence of a primary oxidant, while the formation of **7** stems from competitive direct perhydrolysis.^[33–35]

To obtain deeper insights into the mechanism of the AcMP11-catalyzed detoxification, we synthesized an analog of PhX bearing a quaternary ammonium instead of a tertiary amine as a substituent on the side chain (PhXMe⁺ **11**; Scheme 4-top),^[42] therefore preventing any possible formation of phosphonothioate and aziridinium through the mechanism proposed in Scheme 3. Thus, this compound **11** was engaged for 5 h under conditions A and B that induced the decomposition of PhX (A: AcMP11/H₂O₂/HEPES buffer-MeOH; and B: H₂O₂/HEPES buffer-MeOH) and the reaction was monitored by ³¹P NMR. Under conditions A, no reaction occurred and the starting compound **11** was found unchanged. However, under perhydrolytic conditions B, traces of P–S bond cleavage product **7** were observed as sole decomposition product.

Finally, we also assessed the reactivity of *O,S*-diethyl methylphosphonothioate **12**, which does not bear any nitrogen atom at the end of the *S*-ethyl chain, and that is often claimed as the “most common simulant of VX”. Under both conditions A and B, no reaction occurred after 5 h.

From these results, we thus propose the mechanism depicted in Scheme 4: reaction between hydrogen peroxide and AcMP11 rapidly first generates the peroxospecies **13** that further adds onto the electrophilic phosphorous atom to provide the intermediate species **14**. Then, in the presence of the amino group on the side chain, compound **14** undergoes an internal nucleophilic substitution (S_Ni) to afford **5a** with ejection of the aziridinium **8**. In contrast, without any possibility of nucleophilic displacement through anchimeric assistance,

the reverse addition takes place from **13**, with decomposition of AcMP11 and recovery of starting compounds **11** and **12**. Whereas PhX is used as a racemic mixture of *R*_p and *S*_p isomers, resolution by AcMP11 is rather unlikely: this microperoxidase has only been reported in one enantioselective catalytic transformation (sulfoxidation) with low inductive effects for the trivial thioanisole (20–46% ee).^[43,44]

Conclusions

In conclusion, the oxidative system involving the heme peptide microperoxidase AcMP11 as catalyst and hydrogen peroxide as oxidant decomposes the VX simulant PhX into non-toxic phosphonothioate **5a** as a prominent product. The phosphonothioate is accompanied by trace amounts of P–S and minor amount of P–O bond cleavage products, the latter being also afforded by competitive perhydrolysis path.

According to the usual oxidative detoxification methods, the formation of such phosphonothioate was unexpected, and this new and promising detoxification pathway would not have been discovered through the use of the common VX simulants proposed in the literature. It thus shows the importance of the presence of the aminoethanethiol chain of the V-series nerve agents, not only for their bioactivity but also in the frame of degradation studies. It shall therefore be highly recommended in further studies to use V-series simulants bearing such side chains.

Future work should also be oriented toward the protection of MP11 from competitive oxidative degradation, for example by encapsulation around a protein matrix such as an antibody.^[45]

Experimental Section

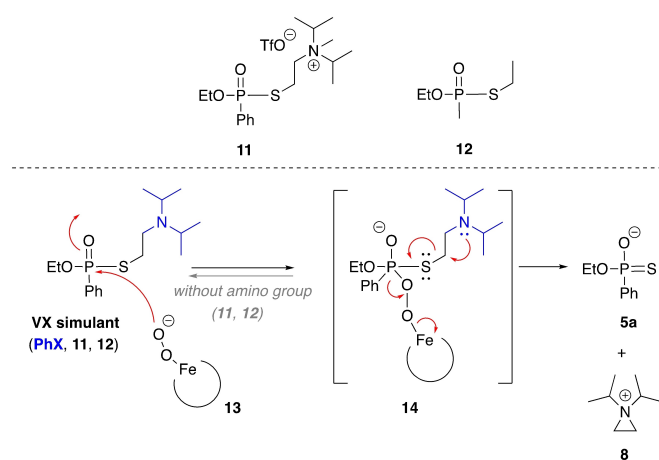
Material

N-Acetylated microperoxidase-11 (AcMP11) was prepared by trypsin digestion of horse-heart cytochrome c (Sigma) as described in the literature.^[46] *N*-Acetylation was performed as previously reported for MP-8.^[47] The heme content was determined by the pyridine chromogen method.^[48] The purity of the sample was assessed to be over 95% based on matrix-assisted laser desorption ionization-time of flight (MALDI-TOF) mass spectrometry analysis.

Preparation of the Solutions

AcMP11. An AcMP11 solution was obtained by solubilizing some milligrams of solid AcMP11 in 1 mL of a buffer solution (pH 8; HEPES 20 mM; 150 mM NaCl). The AcMP11 solution concentration was determined by UV-Vis analysis. A 10 μL aliquot of the AcMP11 solution was added to 2990 μL of a buffer solution (pH 8; HEPES 20 mM; 150 mM NaCl) in a quartz cuvette (1 cm optical path). From the absorbance obtained at 398 nm and Lambert-Beer law (AcMP11 molar absorption at 398 nm: 148000 L mol⁻¹ cm⁻¹) we calculated the exact concentration of AcMP11 0.45 mM).

PhX. A 20 mM PhX solution was obtained by solubilizing a weighted aliquot of neat PhX in methanol. For all reactions, an



Scheme 4. (top) Structures of compounds **11** and **12**; (bottom) Proposed mechanism for the formation of phosphonothioate **5a** from PhX, AcMP11, and H₂O₂.

aqueous solution of hydrogen peroxide (5 mM or 181 mM) was freshly prepared from a 30% aqueous hydrogen peroxide solution, according to the desired concentration.

Kinetic studies (UV-vis). Kinetic degradation studies of PhX were performed by monitoring the changes at the PhX absorption bands (260, 266, and 273 nm). The catalyst oxidation was monitored by the disappearance of the absorption band at 398 nm as a function of time. The reactions were started by adding an aliquot of PhX solution to the methanol/buffer mixture, followed by an aliquot of AcMP11 solution, and then by an aliquot of hydrogen peroxide. Final concentration: PhX 50 or 500 μ M, AcMP11 5 μ M and H₂O₂ 50 μ M. The conditions described above were used unless stated otherwise.

Kinetic studies (³¹P NMR). In an NMR tube, the quantity of simulant (PhX, **11** or **12**) was weighted, followed by the addition of MeOD (240 μ L), buffer solution (pH 8; HEPES 20 mM; 150 mM NaCl) (160 μ L), AcMP11 solution (200 μ L), and the hydrogen peroxide was stepwise added in 5 (10 μ L) aliquots. Final volume: 0.6 mL. Final concentrations: PhX 15 mM, AcMP-11 0.15 mM and H₂O₂ 15 mM. For all reactions, a ³¹P NMR spectrum was recorded before the hydrogen peroxide addition.

Supporting Information

Protocols for the preparation of organophosphorus compounds and neutralization of PhX and characterization (UV, NMR). The authors have cited additional references within the Supporting Information (Ref. [49–52]).

Acknowledgements

This work is part of the DetoxArtMet project funded by the Agence Nationale de la Recherche. This work has been partially supported by Université Rouen Normandie, INSA Rouen Normandie, Centre National de la Recherche Scientifique (CNRS), European Regional Development Fund (ERDF), Labex SynOrg (ANR-11-LABX-0029), Carnot Institute I2 C, the graduate school for research XL–Chem (ANR-18-EUR-0020 XL CHEM), Région Normandie, and BioMedef NBC-5-C-2316.

Conflict of Interests

The authors declare no conflict of interest.

Data Availability Statement

The data that support the findings of this study are available in the supplementary material of this article.

Keywords: organophosphorous nerve agent · biocatalysis · remediation · chemical warfare agent

[1] D. Hafemeister, *Nuclear Proliferation and Terrorism in the Post-9/11 World*, Springer International Publishing, Cham, 2016, pp. 337–351.

- [2] M. Peplow, *Chem. Eng. News* **2018**, 96, 3.
- [3] H. John, M. J. van der Schans, M. Koller, H. E. T. Spruit, F. Worek, H. Thiermann, D. Noort, *Forensic Toxicol.* **2018**, 36, 61–71.
- [4] Annual Report of the OPCW on the Implementation of the Convention on the Prohibition of the Development, Production, Stockpiling and Use of Chemical Weapons and on their Destruction in 2022, C-28/3, Nov. 27th 2023, 1–74.
- [5] J. Nawala, P. Jóźwik, S. Popiel, *Int. J. Environ. Sci. Technol.* **2019**, 16, 3899–3912.
- [6] Y. J. Jang, K. Kim, O. G. Tsay, D. A. Atwood, D. G. Churchill, *Chem. Rev.* **2015**, 115, PR1–PR76.
- [7] K. Kim, O. G. Tsay, D. A. Atwood, D. G. Churchill, *Chem. Rev.* **2011**, 111, 5345–5403.
- [8] B. M. Smith, *Chem. Soc. Rev.* **2008**, 37, 470–478.
- [9] S. Costanzi, J.-H. Machado, M. Mitchell, *ACS Chem. Neurosci.* **2018**, 9, 873–885.
- [10] G. Mercey, T. Verdelet, J. Renou, M. Kliachyna, R. Baati, F. Nachon, L. Jean, P.-Y. Renard, *Acc. Chem. Res.* **2012**, 45, 756–766.
- [11] P. Masson, F. Nachon, *J. Neurochem.* **2017**, 142, 26–40.
- [12] Y.-C. Yang, *Acc. Chem. Res.* **1999**, 32, 109–115.
- [13] T. Islamoglu, Z. Chen, M. C. Wasson, C. T. Buru, K. O. Kirlikovali, U. Afrin, M. R. Mian, O. K. Farha, *Chem. Rev.* **2020**, 120, 8130–8160.
- [14] S. D. Kim, H. Jung, *Ind. Eng. Chem. Res.* **2023**, 62, 6672–6686.
- [15] Y. C. Yang, L. L. Szafraniec, W. T. Beaudry, D. K. Rohrbaugh, *J. Am. Chem. Soc.* **1990**, 112, 6621–6627.
- [16] J. E. Forman, C. M. Timperley, *Curr. Opin. Green Sustain. Chem.* **2019**, 15, 103–114.
- [17] V. B. Silva, Y. H. Santos, R. Hellinger, S. Mansour, A. Delaune, J. Legros, S. Zinoviev, E. S. Nogueira, E. S. Orth, *Green Chem.* **2022**, 24, 585–613.
- [18] H. Targhan, P. Evans, K. Bahrami, *J. Ind. Eng. Chem.* **2021**, 104, 295–332.
- [19] R. A. Sheldon, D. Brady, M. L. Bode, *Chem. Sci.* **2020**, 11, 2587–2605.
- [20] E. L. Bell, W. Finnigan, S. P. France, A. P. Green, M. A. Hayes, L. J. Hepworth, S. L. Lovelock, H. Niikura, S. Osuna, E. Romero, K. S. Ryan, N. J. Turner, S. L. Flitsch, *Nat Rev Methods Primers* **2021**, 1, 1–21.
- [21] E. O'Reilly, M. Corbett, S. Hussain, P. P. Kelly, D. Richardson, S. L. Flitsch, N. J. Turner, *Catal. Sci. Technol.* **2013**, 3, 1490–1492.
- [22] J. Chen, Z. Guo, Y. Xin, Z. Gu, L. Zhang, X. Guo, *Sci. Total Environ.* **2023**, 867, 161510.
- [23] L. F. Serafim, L. Wang, P. Rathee, J. Yang, H. S. Frenk Knaul, R. Prabhakar, *Curr. Opin. Green Sustain. Chem.* **2021**, 32, 100529.
- [24] A. N. Bigley, E. Desormeaux, D. F. Xiang, S. Y. Bae, S. P. Harvey, F. M. Raushel, *Biochemistry* **2019**, 58, 2039–2053.
- [25] A. N. Bigley, M. F. Mabanglo, S. P. Harvey, F. M. Raushel, *Biochemistry* **2015**, 54, 5502–5512.
- [26] I. Cherny, P. Greisen, Y. Ashani, S. D. Khare, G. Oberdorfer, H. Leader, D. Baker, D. S. Tawfik, *ACS Chem. Biol.* **2013**, 8, 2394–2403.
- [27] A. N. Bigley, C. Xu, T. J. Henderson, S. P. Harvey, F. M. Raushel, *J. Am. Chem. Soc.* **2013**, 135, 10426–10432.
- [28] G. Amitai, R. Adani, M. Hershkovitz, P. Bel, I. Rabinovitz, H. Meshulam, *J. Appl. Toxicol.* **2003**, 23, 225–233.
- [29] P.-Y. Renard, H. Schwebel, P. Vayron, L. Josien, A. Valleix, C. Mioskowski, *Chem. Eur. J.* **2002**, 8, 2910–2916.
- [30] B. Picard, I. Chataigner, J. Maddaluno, J. Legros, *Org. Biomol. Chem.* **2019**, 17, 6528–6537.
- [31] S. Mansour, A. Delaune, M. Manneveau, B. Picard, A. Claudel, C. Vallières, L. Sigot, P.-Y. Renard, J. Legros, *Green Chem.* **2021**, 23, 7522–7527.
- [32] A. Delaune, S. Mansour, B. Picard, P. Carrasqueira, I. Chataigner, L. Jean, P.-Y. Renard, J.-C. M. Monbaliu, J. Legros, *Green Chem.* **2021**, 23, 2925–2930.
- [33] Y. C. Yang, L. L. Szafraniec, W. T. Beaudry, C. A. Bunton, *J. Org. Chem.* **1993**, 58, 6964–6965.
- [34] G. W. Wagner, Y.-C. Yang, *Ind. Eng. Chem. Res.* **2002**, 41, 1925–1928.
- [35] G. W. Wagner, *Main Group Chem.* **2010**, 9, 257–263.
- [36] D. Waysbort, E. Manisterski, H. Leader, B. Manisterski, Y. Ashani, *Environ. Sci. Technol.* **2004**, 38, 2217–2223.
- [37] B. Andrae, D. Bauer, P. Gaß, M. Koller, F. Worek, S. Kubik, *Org. Biomol. Chem.* **2020**, 18, 5218–5227.
- [38] Y.-C. Yang, L. L. Szafraniec, W. T. Beaudry, D. K. Rohrbaugh, L. R. Procell, J. B. Samuel, *J. Org. Chem.* **1996**, 61, 8407–8413.
- [39] C. A. S. Brevett, K. B. Sumpter, J. Pence, R. G. Nickol, B. E. King, C. V. Giannaras, H. D. Durst, *J. Phys. Chem. C* **2009**, 113, 6622–6633.
- [40] G. S. Groenewold, J. M. Williams, A. D. Appelhans, G. L. Gresham, J. E. Olson, M. T. Jeffery, B. Rowland, *Environ. Sci. Technol.* **2002**, 36, 4790–4794.
- [41] G. Ilia, M. Petric, E. Bálint, G. Keglevich, *Heteroat. Chem.* **2015**, 26, 29–34.

- [42] S. Elias, I. Columbus, O. Shoshanim, D. Mizrahi, R. Chen, L. Yehezkel, L. Ghindes-Azaria, N. Ashkenazi, Y. Zafrani, *ChemistrySelect* **2022**, *7*, e202201363.
- [43] E. N. Kadnikova, N. M. Kostić, *J. Org. Chem.* **2003**, *68*, 2600–2608.
- [44] S. Colonna, N. Gaggereo, G. Carrea, P. Pasta, *Tetrahedron Lett.* **1994**, *35*, 9103–9104.
- [45] R. Ricoux, E. Lukowska, F. Pezzotti, J. Mahy, *Eur. J. Biochem.* **2004**, *271*, 1277–1283.
- [46] P. A. Adams, R. C. De L. Milton, M. P. Byfield, J. M. Pratt, *J. Inorg. Biochem.* **1988**, *34*, 167–175.
- [47] O. Q. Munro, H. M. Marques, *Inorg. Chem.* **1996**, *35*, 3752–3767.
- [48] J. Aron, D. A. Baldwin, H. M. Marques, J. M. Pratt, P. A. Adams, *J. Inorg. Biochem.* **1986**, *27*, 227–243.
- [49] D. G. Hewitt, *Aust. J. Chem.* **1979**, *32*, 463–464.
- [50] K. E. DeBruin, C. I. W. Tang, D. M. Johnson, R. L. Wilde, *J. Am. Chem. Soc.* **1989**, *111*, 5871–5879.
- [51] A. B. Smith, L. Ducry, R. M. Corbett, R. Hirschmann, *Org. Lett.* **2000**, *2*, 3887–3890.
- [52] L. Briseño-Roa, J. Hill, S. Notman, D. Sellers, A. P. Smith, C. M. Timperley, J. Wetherell, N. H. Williams, G. R. Williams, A. R. Fersht, A. D. Griffiths, *J. Med. Chem.* **2006**, *49*, 246–255.

Manuscript received: February 14, 2024
Revised manuscript received: April 8, 2024
Accepted manuscript online: April 9, 2024
Version of record online: May 10, 2024